

Original Article

Feasibility of 15-Minute Delayed Hepatobiliary Phase Imaging Using a 30 Degree Flip Angle in Gadoteric Acid-Enhanced MRI in the Detection of the Focal Liver Lesion in Cirrhotic Liver

Wanwarang Teerasamit, M.D., Pimpakarn Wongpattaranon, M.D.,
Voraparee Suvannarerg, M.D.*

Abstract

Introduction: Added hepatobiliary phase images (HBI) of gadoteric acid-enhanced MRI improve sensitivity for detection of focal liver lesions (FLLs) due to good liver-to-lesion contrast-to-noise ratios (CNRs). The 20-minute delay time is a standard recommendation to obtain appropriate HBI which producing the best liver-to-lesion CNRs.

Objectives: To compare the liver-to-lesion CNR, contrast ratio (CR), and the sensitivity of FLL detection of a 15-minute delayed HBI using a 30° flip angle (15min-FA30) in gadoteric acid-enhanced MRI with those of a standard 20-minute delayed HBI using 25° FA (20min-FA25) in patient with cirrhotic liver.

Methods: Seventy FLLs from 62 patients who underwent gadoteric acid-enhanced MRI with 15min-FA30 and 20min-FA25 HBI were enrolled. Liver-to-lesion CNRs and CRs were compared between the two groups. Two radiologists independently reviewed the presence of FLLs using a four-point scale and detection sensitivity was calculated.

Results: There was no significant difference in the median CNR of all FLLs on the 15min-FA30 (77.6: IQR; 47.4 - 133.2) and that of the 20min-FA25 (81.5: IQR; 48.2 - 140.0). The mean CR of all FLLs on the 15min-FA30 (0.47 ± 0.16) and 20min-FA25 (0.47 ± 0.17) was no significant difference. There was no significant difference in FLLs detection sensitivity for two readers between 15min-FA30 (91.4% and 97.1%) and 20min-FA25 (92.9% and 97.1%)

Conclusions: The CNRs, CRs and lesion detection sensitivity of shorten delayed HBI with high FA in gadoteric acid-enhanced MRI are comparable with the standard delayed HBI in patient with cirrhotic liver. This result indicates that 15min-FA30 can replace 20min-FA25 that help to reduce the total examination time.

Keywords: Gadoteric acid-enhanced MRI, Hepatobiliary phase imaging, Liver-to-lesion contrast-to-noise ratio, Liver-to-lesion contrast ratio

Volume 2023, Issue 1, Page 25-34

CC BY-NC-ND 4.0 license

<https://asianmedjam.com>

Received: 25 April 2022

Revised: 16 November 2022

Accepted: 30 November 2022

Division of Diagnostic Radiology, Department of Radiology, Faculty of Medicine, Siriraj Hospital, Mahidol University, Bangkok, Thailand

***Corresponding author:** Voraparee Suvannarerg, M.D., Division of Diagnostic Radiology, Department of Radiology, Faculty of Medicine, Siriraj Hospital, Mahidol University, Bangkok, Thailand

Introduction

Nowadays, gadoteric acid-enhanced magnetic resonance imaging (MRI) is widely used for detection of a focal liver lesion (FLL), especially hepatocellular carcinoma (HCC) in the patient with chronic liver disease or cirrhosis. It has an excellent sensitivity for detection of HCC¹ and shows better diagnostic performance than the multiphasic multidetector computed tomography (MDCT).^{2,3}

Gadolinium-ethoxybenzyl diethylenetriaminepentaacetic acid (Gd-EOB-DTPA), also known as gadoteric acid or gadoterate disodium (Primovist®, Bayer Schering Pharma, Germany) is a combined extracellular-hepatobiliary contrast agent for MRI.⁴ This agent combines the properties of a conventional extracellular contrast agent that evaluating tissue vascularity on dynamic study and a hepatobiliary agent that assessing hepatocyte function on delayed hepatobiliary phase images (HBI).⁴ Previous studies^{1,5} have shown that, added hepatobiliary phase images (HBI) with unenhanced images and dynamic study improve sensitivity for detection of HCC. This contrast agent is transported into the normal hepatocytes, that beginning at 1 minute after contrast injection and resulting in increase of liver parenchymal signal intensity (SI) due to shortening of the T1 relaxation time.⁴ Difference in SI between liver parenchyma (higher SI) and the FLL that does not uptake the contrast agent (lower SI), or liver-to-lesion contrast-to-noise ratios (CNRs) is best at delayed 20 minutes after gadoteric acid injection.⁶ Thus, 20-minute delay time is a standard recommendation to obtain appropriate HBI.^{7,8}

However, a 20-minute wait is too long, multiple studies were attempted to reducing delay time for HBI and total examination time. Previous studies⁹⁻¹¹ have shown that decreasing the delay time for HBI to 10 minute is sufficient for FLL detection, especially in patients with normal liver function. But the liver-to-lesion CNR of 10-minute delayed HBI was still lower than the standard 20-minute delayed HBI.

Several studies^{7,8} have found that using high flip angle (FA 30 - 35°) in HBI has been improved both liver-to-lesion CNR and FLL detection. In routine dynamic study, T1-weighted GRE sequence uses small flip angle (10 - 15°) and short repetition time for reduced the total scan time that causing incomplete recovery of longitudinal magnetization.

This effect is more obvious for FLL without gadoteric acid uptake that has a longer T1 relaxation time, compared with shorter T1 relaxation time of normally enhanced liver parenchyma. This difference in residual longitudinal magnetization is amplified by increasing FA.

At the author's institute, we had been used 10-minute delayed HBI with high FA in gadoteric acid-enhanced MRI, but this sequence was not sufficient for improve the lesion-to-liver CNR. Thus, the protocol for HBI has been changed by using 15-minute delayed HBI with high flip angle (30°) and standard 20-minute delayed HBI. The purpose of this study was to compare the liver-to-lesion CNR, contrast ratio (CR) and sensitivity of lesion detection of a 15-minute delayed HBI using 30° FA in gadoteric acid-enhanced MRI with those of a standard 20-minute delayed HBI in patient with cirrhotic liver, to evaluate feasibility of shortening of examination time with maintained image quality.

Methods

Study Populations and Standard of Reference

The present retrospective study was approved by the Institutional Ethic Committee, and informed consent was waived. Between March 2018 and December 2020, 978 consecutive patients with cirrhotic liver (aged above 18 years) who had the FLLs that do not uptake gadoteric acid on HBI of gadoteric acid-enhanced MRI (seen as low signal intensity lesion). Nine hundred and sixteen of 978 patients were excluded from the study by the following reasons: incomplete studies/images, poor quality MR images, lesions categorized as cyst, lack of pathologic confirmation or follow-up imaging by CT or MRI performed at least one year after initial MR imaging, known cases of HCC with treatment history of transarterial chemoembolization (TACE) or radiofrequency ablation (RFA). The remaining 62 patients were enrolled in this study (41 males (66.1%) and 21 females (33.9%), age range 31 to 89 years, mean age 63.61 years). All patients had cirrhotic liver, diagnosed by the combination of clinical settings, laboratory evidence and radiologic findings. Twenty-seven patients (27/62, 43.5%) had chronic hepatitis B-related cirrhosis, twenty-two (22/62, 35.5%) had chronic hepatitis C-related cirrhosis, six (6/62, 9.7%) had NASH (non-alcoholic steatohepatitis)-induced cirrhosis, five (5/62, 8.1%) had alcoholic-related cirrhosis and the remaining

two (2/62, 3.2%) had hemochromatosis-related cirrhosis. Child-Pugh A cirrhosis were found in 53 patients (85.5%) and Child Pugh B cirrhosis were found in 9 patients (14.5%).

Seventy FLLs were found in 62 patients, including 62 FLLs that were HCCs (62/70, 88.6%) (size range 0.8 - 6.2 cm, mean size 1.84 cm). A diagnosis of HCC was based on pathological examination (n = 3, 4.8%), typical HCC hallmarks on dynamic gadoteric-enhanced MRI (arterial hyperenhancement and portovenous or delayed phase washout) (n = 38, 61.3%), and progression of the disease as depicted at 6-monthly follow up imaging (n= 21, 33.9%). The remaining 8 of 70 nodules were benign lesions (8/70, 11.4%) (size range 0.6 - 4.7 cm, mean 1.77 cm). A diagnosis of benign lesions was made by pathological examination (n = 2, 25%) and no interval change or less conspicuous without treatment at follow-up imaging (CT or MRI) at least one year after initial imaging (n = 6, 75%)

MR Examination

All studies were performed by using 3.0-T scanner (Magnetom Vida, Siemens Healthineers, Germany), or 3.0-T scanner (Signa Architect, GE Healthcare, USA), or 3.0-T whole-body MR system (Ingenia 3.0-T and Achieva 3.0-T; Philips Healthcare, the Netherlands) with phased-array coils. The MRI examination comprised of axial dual-echo T1-weighted gradient-echo sequence and axial T2-weighted turbo spin echo sequences with and without fat suppression. The dynamic study and delayed

HBI were performed with 3D axial fat suppressed T1-weighted gradient-echo sequences. The dynamic study was done during suspended respiration at 30 seconds (arterial phase), 70 seconds (portovenous phase), 120 seconds and delayed 5 minutes (transition phases) after intravenous contrast injection. A 30° flip angle was used for 15-minute delayed HBI (15min-FA30) and a 25° FA was used for 20-minute delayed HBI (20min-FA25). Gadoteric acid (Primovist®; Bayer-Schering Healthcare, Berlin, Germany) was administered at 0.1 mL/kg in dose (equivalent to 25 µmol/kg) and 1.5 mL/s in rate through an antecubital vein and were flushed with 30 mL NSS at the same rate.

Image Analysis

Quantitative Analysis

The quantitative analysis was performed by a radiologist with 13 years of liver MRI experience. The signal intensity (SI) of the liver parenchyma and each FLL were measured on two HBIs (15min-FA30 and 20min-FA25). Background image noise was measured ventral to the liver outside of the patient's body (Figure 1). The liver-to-lesion contrast-to-noise ratio (CNR) and contrast ratio (CR) were calculated for each image as follows:

$$\text{CNR} = (\text{SI Liver} - \text{SI Lesion}) / \text{SD Noise}$$

$$\text{CR} = (\text{SI Liver} - \text{SI Lesion}) / \text{SI Liver}$$

Where, SI Liver is the mean SI of the liver parenchyma, SI Lesion is the mean SI of FLL, and SD Noise is the mean standard deviation of the background image noise.

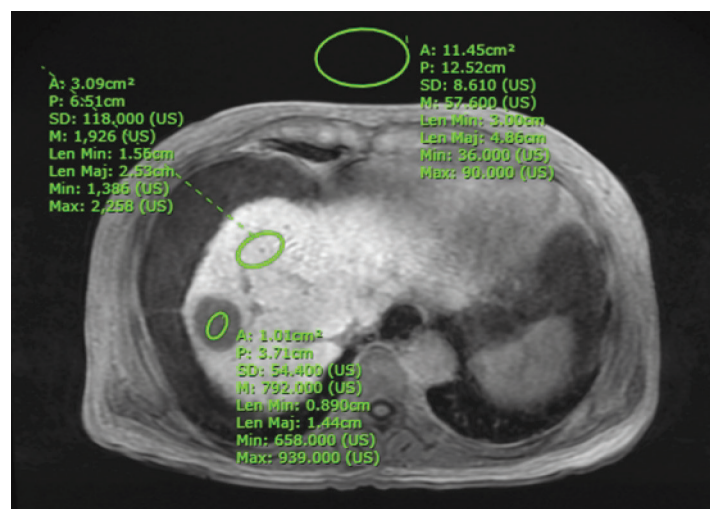


Figure 1 The measurement of signal intensity of liver parenchyma, focal liver lesion and background image noise for each lesion on both hepatobiliary phase images.

The diameter of each FLL was measured on the 20min-FA25 HBI. All FLLs were classified as large (short axis ≥ 10 mm) or small lesions (short axis < 10 mm). Sixty-two lesions (62/70, 88.6%) were categorized as large lesions (size range 1 - 6.2 cm, mean 1.97 cm) and eight lesions (8/70, 11.4%) were classified as small lesions (size range 0.6-0.9 cm, mean 0.8 cm).

Qualitative Analysis

The two HBIs (15min-FA30 and 20min-FA25) were independently and randomly reviewed by two radiologists with 13 years and 10 years of experience in liver MRI. These two readers were blinded to the clinical information, pathological information, follow up MRI interpretations and the final diagnosis. All images were evaluated on picture archiving and communication system (PACs). The reviewers evaluated the presence of FLL using a four-point scale as follows (depend on the presence of the lesion): 1 = definitely absent, 2 = probably absent, 3 = probably present, 4 = definitely present. The reviewers marked FLLs using arrows and scales on PACs and a coordinator with in-training last year resident matched them to the reference standard.

Statistical Analysis

Statistical software (SPSS 18: SPSS, Chicago, IL, USA) was used for all statistical analyses. The liver-to-lesion CNR that showed non-normal distribution and CR showed normal distribution were compared by Wilcoxon's signed-rank test and paired t test, respectively for quantitative analysis. For the calculation of the sensitivity of the lesion detection for all FLLs, 3 and 4-point

scale were considered positive and 1 and 2-point scale were considered negative. The McNemar test was used to compare the detection sensitivities for FLLs between 15min-FA30 and 20min-FA25. A *P*-value of less than .05 was considered to indicate statistical significance. Inter-reader agreement was assessed by weighted Cohen's Kappa statistic.

Results

The liver-to-lesion CNRs and CRs on the two HBIs are shown in Figures 2 and 3, and Table 1. For all focal liver lesions, the median of the CNR from 15min-FA30 and 20min-FA25 were 77.6 and 81.5, respectively which showed no significant difference (*P* = .089). The mean of the CR from 15min-FA30 and 20min-FA25 were 0.47 ± 0.16 and 0.47 ± 0.17 , respectively which showed no significant difference (*P* = .353).

For each subgroup, small and large sizes, benign nodules and HCCs and Child-Pugh A and B cirrhosis also showed no significant difference of the CNRs and CRs in both HBIs.

No significant difference of the CNRs and CRs from 15min-FA30 compared to 20min-FA25 in the small size subgroup (*P* = .735 and *P* = .650) and the large size subgroup (*P* = .067 and *P* = .405).

No significant difference of the CNRs and CRs from 15min-FA30 compared to 20min-FA25 in the benign lesion subgroup (*P* = .612 and *P* = .332) (Figure 4) and HCCs subgroup (*P* = .055 and *P* = .471) (Figure 5).

No significant difference of the CNRs and CRs from 15min-FA30 compared to 20min-FA25 in the Child-Pugh A cirrhosis subgroup (*P* = .068 and *P* = .504) and the Child-Pugh B cirrhosis subgroup (*P* = .767 and *P* = .372).

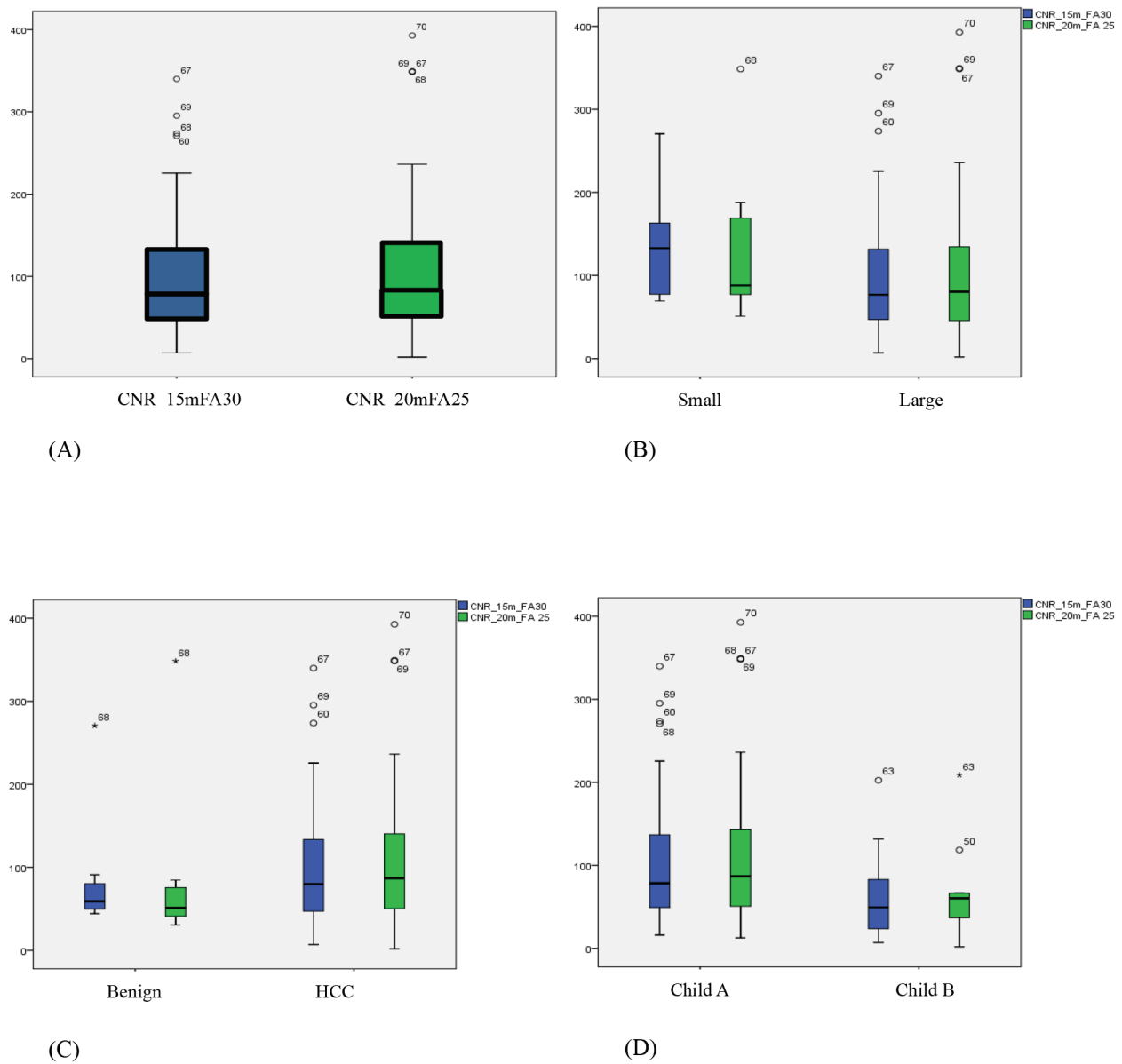


Figure 2 Box and Whisker plot charts of the CNRs from 15min-FA30 and 20min-FA25 in (A) all lesions and each subgroup, (B) small and large size of lesions, (C) benign lesions and HCC, and (D) cirrhosis Child-Pugh class A and B.

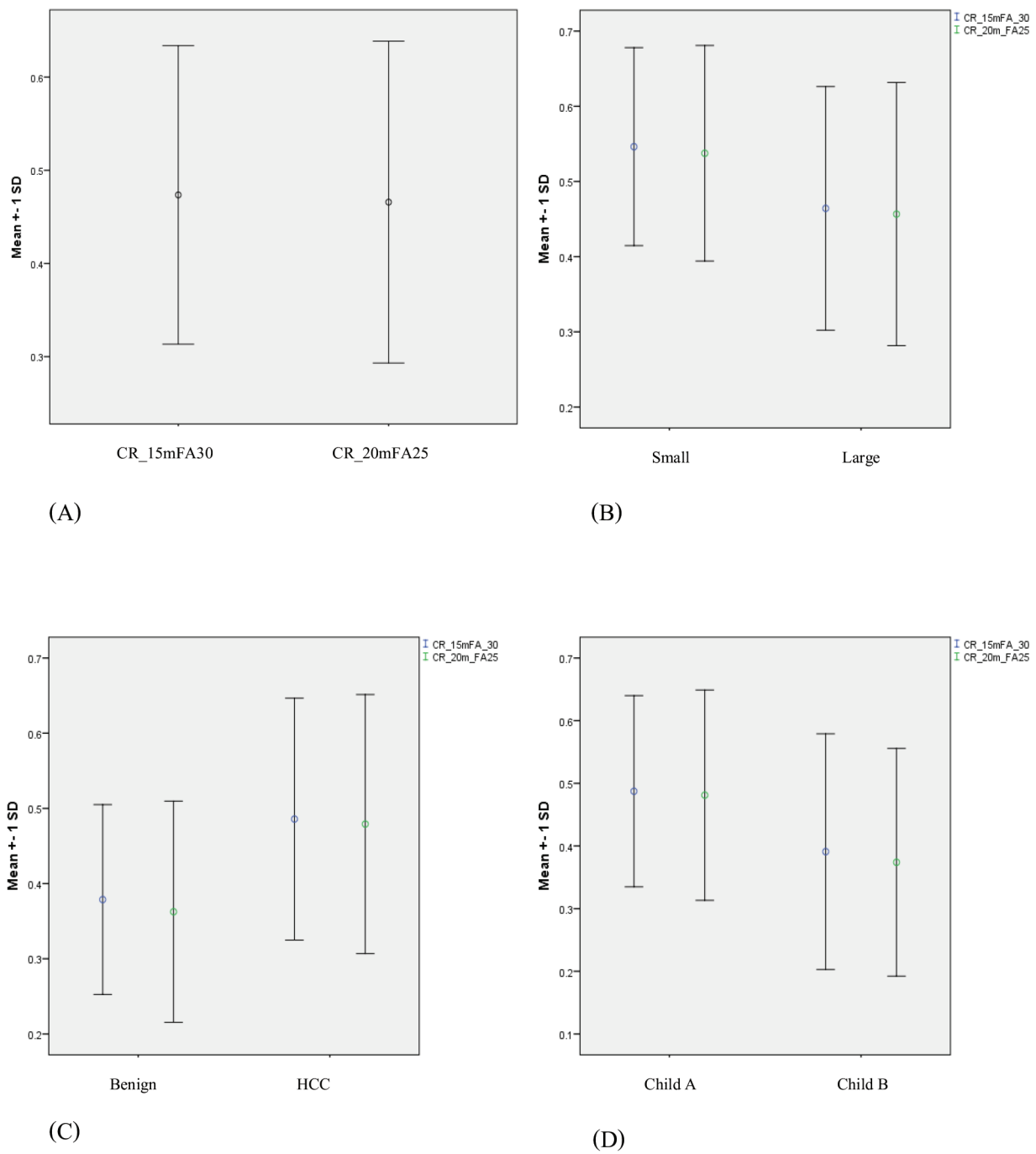
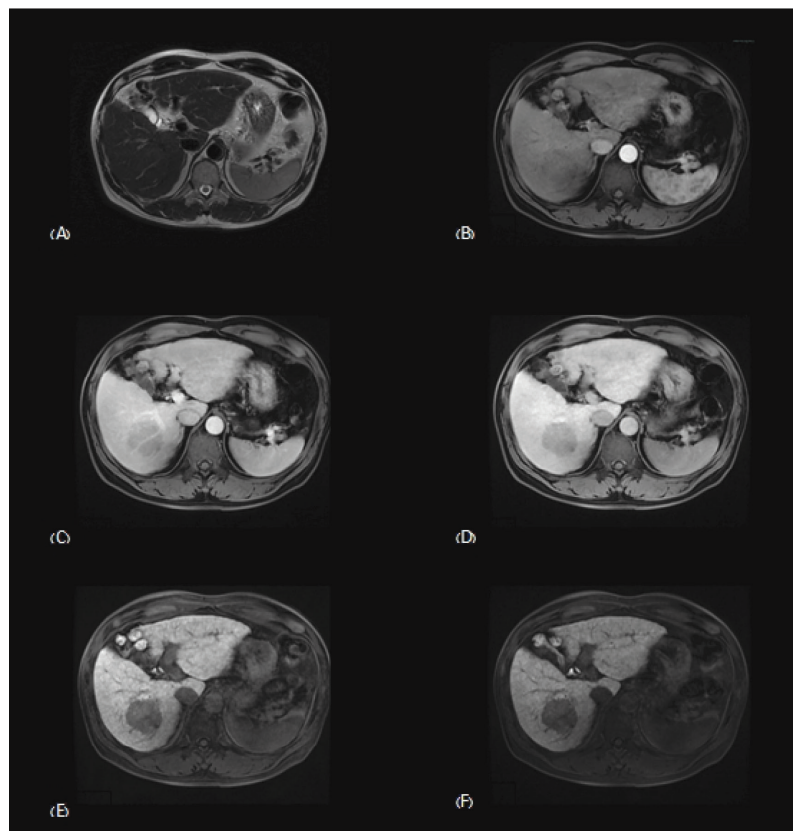


Figure 3 Error bar charts of the CRs from 15min-FA30 and 20min-FA25 in (A) all lesions and each subgroup, (B) small and large size of lesions, (C) benign lesions and HCCs, and (D) cirrhosis Child-Pugh class A and B.

Table 1 The median (P25, P75) of the CNRs and the mean of the CRs from both HBI (15min-FA30 and 20min-FA25) in each subgroup

| | Total | | | Total | | |
|--------------------------------|------------------------|-----------------------|---------|------------------|-----------------|---------|
| | Median CNR (P25, P75) | | | Mean CR \pm SD | | |
| | 15min-FA30 | 20min-FA25 | P-value | 15min-FA30 | 20min-FA25 | P-value |
| All lesions (N = 70) | 77.6 (47.4, 133.2) | 81.5 (48.2, 140.0) | .089 | 0.47 \pm 0.16 | 0.47 \pm 0.17 | .353 |
| Size | | | | | | |
| Small (N = 8) | 132.9 (77.2, 170.0) | 88.1 (76.8, 187.5) | .735 | 0.55 \pm 0.13 | 0.54 \pm 0.14 | .650 |
| Large (N = 62) | 76.9 (46.3, 131.8) | 80.5 (45.5, 135.8) | .067 | 0.46 \pm 0.16 | 0.46 \pm 0.17 | .405 |
| Characteristic lesion | | | | | | |
| Benign (N = 8) | 59.1 (49.4, 91.0) | 51.1 (38.2, 84.7) | .612 | 0.38 \pm 0.13 | 0.36 \pm 0.15 | .332 |
| HCC (N = 62) | 79.8 (47.2, 135.2) | 86.8 (50.2, 142.0) | .055 | 0.48 \pm 0.16 | 0.48 \pm 0.17 | .471 |
| Cirrhosis child pugh | | | | | | |
| Class A (N = 60) | 78.5 (49.2, 138.4) | 86.8 (50.4, 145.4) | .068 | 0.49 \pm 0.15 | 0.48 \pm 0.17 | .504 |
| Class B (N = 10) | 49.4 (22.3, 107.3) | 60.4 (31.2, 92.6) | .767 | 0.39 \pm 0.19 | 0.37 \pm 0.18 | .372 |

**Figure 4** A 60-year-old male with chronic hepatitis B cirrhosis had pathologically proven large regenerative nodule at hepatic segment VI. Gadoxetic acid-enhanced liver MRI revealed a 4.7 cm well-defined nodule at hepatic segment VI which showed isoSI on T2Wi (A), no enhancement on arterial phase (B), hypoSI on portovenous phase (C), and transition phase (D). (E) and (F) showed hypoSI on 15min-FA30 and 20min-FA25 HBIs, respectively.

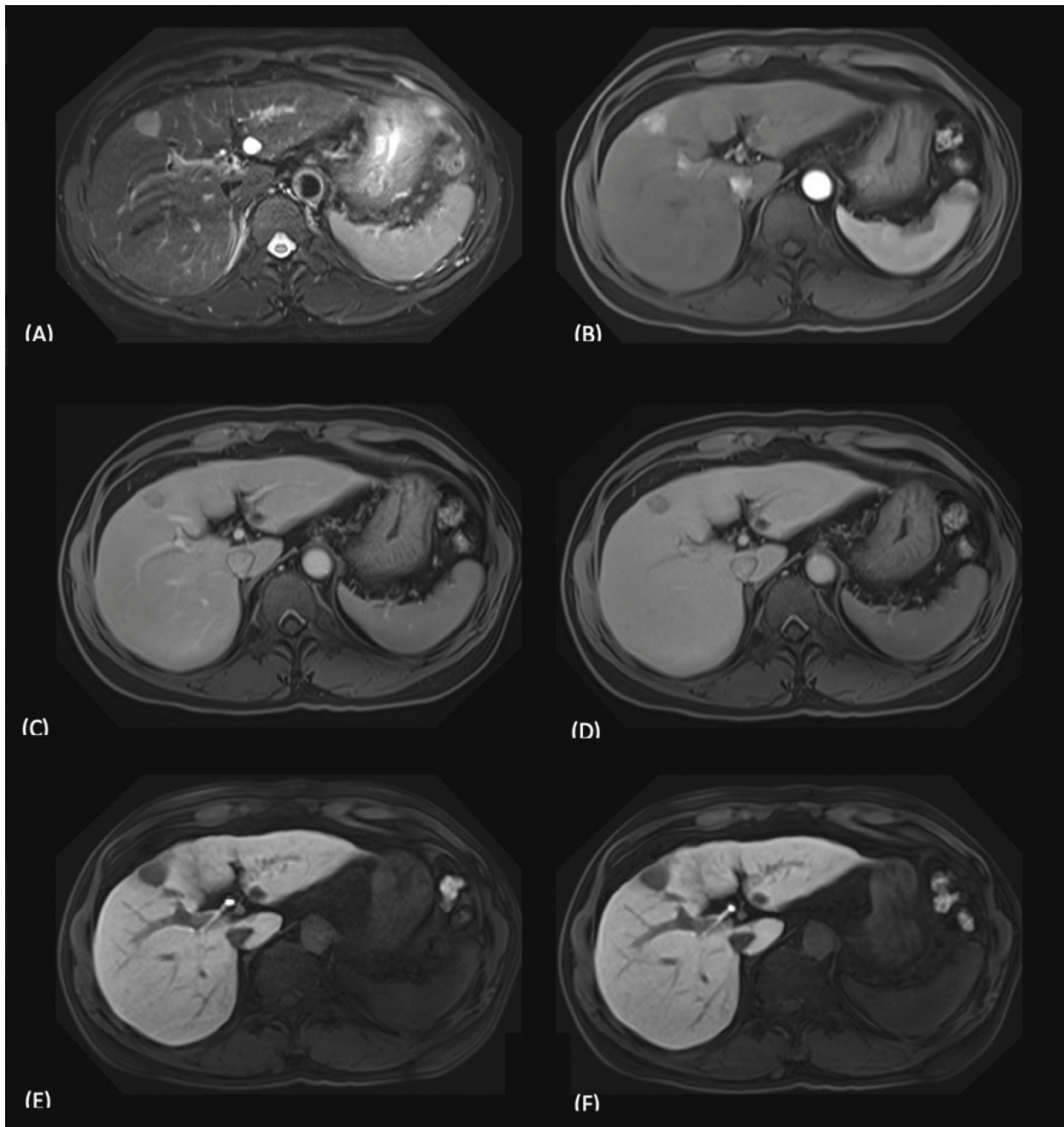


Figure 5 A 56-year-old male with chronic hepatitis C cirrhosis and pathologically proven HCC at hepatic segment IVb/V. Gadoteric acid enhanced liver MRI revealed a 1.7 cm well-defined nodule at hepatic segment IVb/V which showed hyperSI on T2W (A) with arterial enhancement (B) and washout on portovenous (C) and transition phases (D). (E) and (F) showed hypoSI on 15min-FA30 and 20min-FA25 HBIs, respectively.

For all focal liver lesions, the sensitivity of the lesion detection in 15min-FA30 was 91.4% and 97.1% from the first and the second readers, respectively. While in 20min-FA25 was 92.9% from the first reader and 97.1% from the second reader (Table 2). There was no significant difference in

the detection sensitivity between 15min-FA30 and 20min-FA25 for both readers. Inter-reader agreement in 15min-FA30 and 20min-FA25 were 0.52 and 0.441, respectively that indicate moderate agreement.

Table 2 The sensitivity of the lesion detection for all lesions and each subgroup by both readers

| | Reader 1 (%) | | Reader 2 (%) | |
|---------------------|----------------------|----------------------|----------------------|----------------------|
| | 15m-FA30 (95%CI) | 20m-FA25 (95%CI) | 15m-FA30 (95%CI) | 20m-FA25 (95%CI) |
| All lesions | 91.4 (82.3, 96.8) | 92.9 (84.1, 97.6) | 97.1 (90.1, 99.7) | 97.1 (90.1, 99.7) |
| Small | 87.5 (47.4, 99.7) | 87.5 (47.4, 99.7) | 100 (63.1, 100) | 100 (63.1, 100) |
| Large | 91.9 (82.2, 97.3) | 93.6 (84.3, 98.2) | 96.8 (88.8, 99.6) | 96.8 (88.8, 99.6) |
| Benign | 75 (34.9, 96.8) | 75 (34.9, 96.8) | 87.5 (47.4, 99.7) | 87.5 (47.4, 99.7) |
| HCC | 93.6 (84.3, 98.2) | 95.2 (86.5, 99.0) | 98.4 (91.3, 100) | 98.4 (91.3, 100) |
| Child-Pugh A | 93.3 (83.8, 98.2) | 95.0 (86.1, 99.0) | 98.3 (91.1, 100) | 98.3 (91.1, 100) |
| Child-Pugh B | 80.0 (44.4, 97.5) | 80.0 (44.4, 97.5) | 90.0 (55.5, 99.8) | 90.0 (55.5, 99.8) |

(95% CI = 95% confidence interval)

Discussion

Although, the previous study⁷ have found that the diagnostic performance of 10-minute delayed HBI with a high FA (30°) was similar to or higher than the standard 20-minute delayed HBI with both low (10°) and high (30°) FAs. But the CNRs for HCCs on 10min-FA30 was still lower than that of 20min-FA30. The main populations of this previous study⁷ were Child-Pugh A cirrhosis. Patients with Child-Pugh A cirrhosis showed strong liver parenchymal enhancement on 20-minute delayed HBI.¹² As compared with the non-cirrhotic liver, the cirrhotic liver may have decreased parenchymal enhancement in the hepatobiliary phase and the time to peak enhancement may be delayed, due to deterioration of hepatocyte function for gadoxetic acid uptake.⁴ So, 10-minute delay time in compensated cirrhotic liver might be too short to delay for appropriate liver parenchymal enhancement on HBI. However, in the previous literature¹² have shown that patients with Child-Pugh B or C cirrhosis do not have an increase of liver parenchymal enhancement after 8 or 10 minutes after gadoxetic acid administration. Thus, in cases of patient with decompensated cirrhosis (Child-Pugh B or C), 20-minute delayed HBI was not necessary.

The present study has found that 15min-FA30 were comparable with the standard 20min-

FA25 HBI of gadoxetic acid-enhanced MRI in patients with a cirrhotic liver. There was no significant difference in CNRs, CRs, and the lesion detection sensitivity between two images sequences on all FLLs and all subgroups (benign lesions and HCCs, small and large lesions, Child-Pugh A and B cirrhosis). Most of the populations in this study were Child-Pugh A cirrhosis (85.5%), as aforementioned, this group should have strong liver parenchymal enhancement on 20-minute delayed HBI.¹² Thus, the result indicates that 15min-FA30 can potentially replace 20min-FA25 HBI of gadoxetic acid-enhanced MRI in cirrhotic liver.

Even though, there is increasing the CNR of the non-gadoxetic uptake tumor in the liver when using a high FA. But specific absorption rate (SAR) is also enhanced, causing energy deposition in the patient's body by radiofrequency (RF) pulses, especially high field strength MR scanner (3.0 T).^{7,13} This effect should be concerned and aware.

There are several limitations in this study. First, this study was retrospective and there was a difference in MRI scanners. Second, there was a small sample size that may affect the statistical results. Third, in the quantitative analysis, smaller lesions are affected more by the partial volume effect to measure SI and more limited for drawing ROI.

In conclusion, the CNRs, CRs, and the lesion detection sensitivity of shorten delayed HBI with high FA (15min-FA30) in gadoxetic acid-enhanced MRI are comparable with standard delayed HBI (20min-FA25) in patient with cirrhotic liver. This result indicates that 15min-FA30 can potentially replace 20min-FA25 that help to reduce the total examination time.

References

1. Teerasamit W, Tongdee R, Yodying J. Diagnostic performance of gadoxetic acid-enhanced MR imaging in the diagnosis of hepatocellular carcinoma in cirrhotic Liver. *J Med Assoc Thai*. 2017;100(8):918-926.
2. Hwang J, Kim SH, Lee MW, Lee JY. Small (≤ 2 cm) hepatocellular carcinoma in patients with chronic liver disease: comparison of gadoxetic acid-enhanced 3.0 T MRI and multiphasic 64-multirow detector CT. *Br J Radiol*. 2012;85(1015):314-322.
3. Onishi H, Kim T, Imai Y, et al. Hypervascular hepatocellular carcinomas: detection with gadoxetate disodium-enhanced MR imaging and multiphasic multidetector CT. *Eur Radiol*. 2012;22(4):845-854.
4. Cruite I, Schroeder M, Merkle EM, Sirlin CB. Gadoxetate disodium-enhanced MRI of the liver: part 2, protocol optimization and lesion appearance in the cirrhotic liver. *AJR Am J Roentgenol* 2010;195(1):29-41.
5. Ahn SS, Kim MJ, Lim JS, Hong HS, Chung YE, Choi JY. Added value of gadoxetic acid-enhanced hepatobiliary phase MR imaging in the diagnosis of hepatocellular carcinoma. *Radiology*. 2010;255(2):459-466.
6. Frericks BB, Loddenkemper C, Huppertz A, et al. Qualitative and quantitative evaluation of hepatocellular carcinoma and cirrhotic liver enhancement using Gd-EOB-DTPA. *AJR Am J Roentgenol*. 2009;193(4):1053-1060.
7. Jeon I, Cho ES, Kim JH, Kim DJ, Yu JS, Chung JJ. Feasibility of 10-minute delayed hepatocyte phase imaging using a 30° flip angle in Gd-EOB-DTPA-enhanced liver MRI for the detection of hepatocellular carcinoma in patients with chronic hepatitis or cirrhosis. *PLOS ONE*. 2016;11(12):0167701.
8. Lee D, Cho ES, Kim DJ, Kim JH, Yu JS, Chung JJ. Validation of 10-minute delayed hepatocyte phase imaging with 30° flip angle in gadoxetic acid-enhanced MRI for the detection of liver metastasis. *PLOS ONE*. 2015;10(10):0139863
9. Motosugi U, Ichikawa T, Tominaga L, et al. Delay before the hepatocyte phase of Gd-EOB-DTPA-enhanced MR imaging: Is it possible to shorten the examination time? *Eur Radiol*. 2009;19(11):2623-2629
10. van Kessel CS, Veldhuis WB, van den Bosch MA, van Leeuwen MS. MR liver imaging with Gd-EOB-DTPA: a delay time of 10 minutes is sufficient for lesion characterization. *Eur Radiol*. 2012;22(10):2153-2160.
11. Sofue K, Tsurusaki M, Tokue H, Arai Y, Sugimura K. Gd-EOB-DTPA-enhanced 3.0 T MR imaging: quantitative and qualitative comparison of hepatocyte-phase images obtained 10 min and 20 min after injection for the detection of liver metastases from colorectal carcinoma. *Eur Radiol*. 2011;21(11):2336-2343.
12. Verloh N, Haimerl M, Rennert J, et al. Impact of liver cirrhosis on liver enhancement at Gd-EOB-DTPA enhanced MRI at 3 Tesla. *Eur J Radiol*. 2013;82(10):1710-1715.
13. Bashir MR, Merkle EM. Improved liver lesion conspicuity by increasing the flip angle during hepatocyte phase MR imaging. *Eur Radiol*. 2011;21(2):291-294.